Experimental Evaluation of Voltage Resonance on Industrial Cables

Tamiris Grossl Bade, James Roudet, Jean-Michel Guichon, Patrick Kuo-Peng, and Carlos Sartori *Senior Member, IEEE*

***Abstract*—This paper considers the resonance phenomena observed on cables connected to power converters, evaluating theoretically and experimentally the voltage amplification due to resonance on these cables. The experimental study was effectuated on cables typically used on industrial applications. Factors restricting resonance-due amplifications are considered, as well as the conditions under which resonance issues may rise in such systems.**

***Index Terms*—Multiconductor transmission line, Transmission line resonance, EMC of Power Converters.**

I. Introduction

CABLE resonance is a well-known phenomenon that may considerably compromise an electrical installation safety. Numerous applications where cable resonance causes system dysfunctions can be found in the literature, e.g. connections between motors and its drivers [1]–[4], feeding line of high speed trains [5], connections between offshore generator stations and onshore electrical substations [6]–[8].

In all these examples the connections under study include long electric cables. Problems rise when the switching harmonics generated by power converters excite the cable at its natural frequencies [1]. It is actually very likely that cables a few meters long will resonate, as will be shown in section III-C.

Estimating the actual over-voltage amplitude in power cables in such conditions is the main goal of this paper. A theoretical model capable of correctly predict such over-voltages will allow the development and sizing of efficient protection techniques, such as usage of filters, impedance matching, etc. Also, factors limiting resonance-due voltage amplifications are studied.

In this context, power cables traditionally used on industrial applications were chosen to be characterized and modeled. The chosen characterization method obtains the cable parameters in function of frequency. A frequency-domain model capable of predicting the voltages and currents steady-state behavior all along the cable is detailed, and its results are experimentally verified. This model can be used on a time-domain application with the decomposition of the input voltage/current in a Fourier series, followed by the system simulation for each individual harmonic at its own frequency and the reconstruction of the results on time-domain according to the Fourier series definition.

In order to represent the power converters switching harmonics on frequency domain, thus being able to define these harmonics as the line's excitation source on the model just described, the equivalent source model found in [9], [10] will be used.

This paper is organized as follows: section II introduces the frequency-domain model , section III describes the experimental study on the cable resonance, and in section IV a time-domain application is considered.

Tamiris G. Bade, James Roudet, and Jean-Michel Guichon are with the Univ. Grenoble Alpes, CNRS, Grenoble INP, G2Elab, 38000 Grenoble, France

Patrick Kuo-Peng is with the Federal University of Santa Catarina, Florianópolis, Brazil

C. A. F. Sartori is with Escola Politécnica da Universidade de São Paulo (PEA/EPUSP), São Paulo 05508-010, SP, Brazil, with Instituto de Pesquisas Energéticas e Nucleares (IPEN/CNEN-SP),São Paulo 05508-900, SP, Brazil,

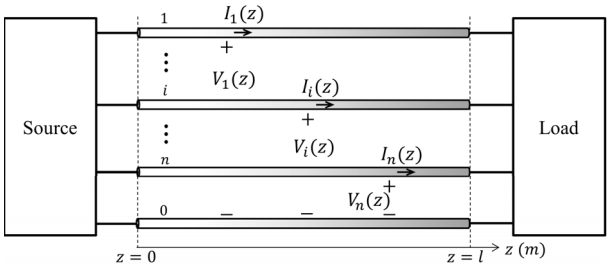

Fig. 1: Generic multi-conductor transmission line

II. Cables as Transmission-Lines

This section introduces the frequency-domain model, which is based on the multi-conductor transmission line (MTL) chain matrix modeling [11]. Consider the $n+1$ conductors transmission line shown in Fig. 1. The classical MTL equations derive from the well-known telegrapher equations, written in matrix form and in the frequency-domain as follows:

$$\frac{d}{dz}\mathbf{V}(z) = -\mathbf{Z}\,\mathbf{I}(z) \tag{1}$$

$$\frac{d}{dz}\mathbf{I}(z) = -\mathbf{Y}\,\mathbf{V}(z) \tag{2}$$

Where $\mathbf{V}$ and $\mathbf{I}$ are vectors of size n containing respectively the phasor voltages and currents of each active conductor related to the reference conductor. The $n\times n$ matrices $\mathbf{Z} = \mathbf{R}+j\omega\mathbf{L}$ and $\mathbf{Y} = \mathbf{G} + j\omega\mathbf{C}$ contain the cable self and mutual per-unit-length impedances and admittances, respectively;j is the imaginary unity and ω is the angular frequency. The definition of $\mathbf{R}$ (linear resistances), $\mathbf{L}$ (linear inductances),$\mathbf{G}$ (linear conductances), and $\mathbf{C}$ (linear capacitances) can be found in [11]. For a $n + 1 = 2$ conductor line these equations are scalar, as well as these parameters.

The terminal conditions of the line in Fig. 1 are defined as:

$$\mathbf{V}(0) = \mathbf{Z}_S\mathbf{I}(0) \tag{3}$$

$$\mathbf{V}(l) = \mathbf{Z}_L \mathbf{I}(l) \tag{4}$$

The voltages an currents along the line can be written in function of its inputs using the MTL chain matrix model defined in [11]:

$$\begin{bmatrix} \mathbf{V}(z) \\ \mathbf{I}(z) \end{bmatrix} = \begin{bmatrix} \mathbf{\Phi}_{11}(z) & \mathbf{\Phi}_{12}(z) \\ \mathbf{\Phi}_{21}(z) & \mathbf{\Phi}_{22}(z) \end{bmatrix} \begin{bmatrix} \mathbf{V}(0) \\ \mathbf{I}(0) \end{bmatrix} \tag{5}$$

$$\mathbf{\Phi}_{11}(z) = \mathbf{Z}_c \cosh(z\sqrt{\mathbf{YZ}})\mathbf{Y_c} \tag{6}$$
$$\mathbf{\Phi}_{12}(z) = -\mathbf{Z}_c \sinh(z\sqrt{\mathbf{YZ}}) \tag{7}$$
$$\mathbf{\Phi}_{21}(z) = -\sinh(z\sqrt{\mathbf{YZ}})\mathbf{Y_c} \tag{8}$$
$$\mathbf{\Phi}_{22}(z) = \cosh(z\sqrt{\mathbf{YZ}}) \tag{9}$$

$\mathbf{Z}_c$ is the characteristic impedance matrix,$\mathbf{Y}_c = \mathbf{Z}_c^{-1}$ is the characteristic admittance matrix and $\mathbf{\Gamma} = \sqrt{\mathbf{YZ}}$ is the non-diagonalized propagation matrix. These line parameters matrices are obtained from the characterization of the power cable under study. This characterization was performed with an impedance analyzer following the method described in [12], and by connecting the cable to the analyzer through a balun transformer, to avoid measurement errors due to parasitic-currents.

The input currents $\mathbf{I}(0)$ and voltages $\mathbf{V}(0)$ can be found by re-injecting equations (3) and (4) in eq. (5) evaluated at $z = l$. Thus, voltages $\mathbf{V}(z)$ and currents $\mathbf{I}(z)$ can be calculated from (5). This solution is the frequency-domain model.

III. Experimental analysis

The goal of this paper is to determine experimentally the actual voltage amplification due to resonance in a power cable. To that end, an experiment consisting on the line voltage measurement, for different excitation frequencies, on the position of the line z_M where the maximum voltage occurs once resonance is established (Figs. 3 and 6) was implemented. Note that for frequencies other than the line's natural frequencies f_n, the line's maximum voltage may be positioned elsewhere, and won't necessarily be measured.

In order to maximize reflection on the source terminal an AB-class push-pull amplifier with closed loop was used to emulate a voltage source V_s with very low output impedance. This way total reflection occurs on the source end, the source reflection coefficient Γ_S being

$$\Gamma_S = \frac{Z_c - Z_S}{Z_c + Z_S} = 1 \tag{10}$$

A battery-powered scope was used for the voltage measurements, thus avoiding alternative current paths through the scope's feeding cable. Also, the probe equivalent impedance was taken in account in the theoretical model because it interferes slightly in the measured voltage.

The experiment results are detailed in the following subsection. The subsequent sections discuss the impact of losses on the voltage amplification and, afterwards, the voltage amplification bandwidth and its implications.

Source: http://www.caledonian-cables.co.uk

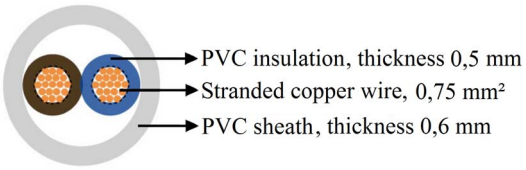

Fig. 2: Cross-section of the two-conductor cable used in the resonance experiment

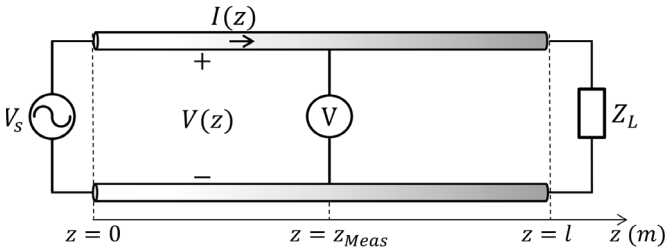

Fig. 3: Schematics of the two-conductor line resonance experiment

A. Results

The experiment just described was performed for two and three-conductor power cables, both $12m$ long and encapsulated sheaths that guarantee the conductors are equally distant from one another along the line.

The two-conductor cable H03VVH2-F was chosen for the experiment, its cross-section is presented in Fig. 2. The conductors are stranded copper wires of section $0,75mm^2$, surrounded by a PVC sheath. The experiment schematic is in Fig. 3

The experimental results are plotted against the theoretical solution, obtained as described in section II, in terms of the voltage amplification $V(z_M)/V_s$.

The experiment was effectuated for an open-ended line (Fig. 4a), a short-circuited line (Fig. 4b) and a line ended by a more realistic LC load (4c), consisting in the parallel association of a $L = 0.43mH$ inductor with a $C = 1nF$ capacitor.

The frequency-domain model presents a good agreement with the experimental data. Furthermore, the analysis show that line resonance may amplify the input voltage signal up to 11 times around its natural frequency for a standard two-conductor cable with parallel LC load.

For the three-conductor line the cable Titanex H07RN-F 3G2,5 was chosen, a cable often used to feed monophasic high power devices on industrial applications, its cross section is represented in Fig. 5. It is composed of three stranded copper wires of section $2,5mm^2$ insulated by elastomer sheaths. The experiment schematics is in Fig. 6.

Again, the experimental data and the theoretical model results are ploted in terms of the voltage amplification $V_1(z_M)/V_s$ on Fig. 7.

The three-conductor line presents voltage amplifications up to 10 times the input signal.

Definitely, open-ended and short-circuited lines are not likely to be found on industrial systems (and if they're found, EMI problems would not be our first concern). However, Fig.

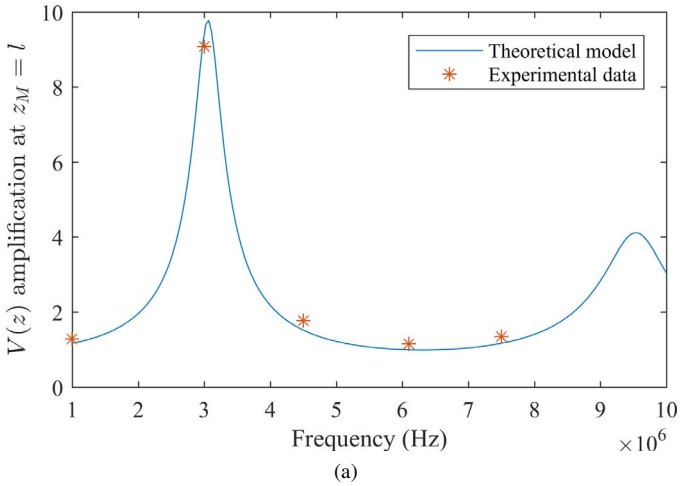

(a)

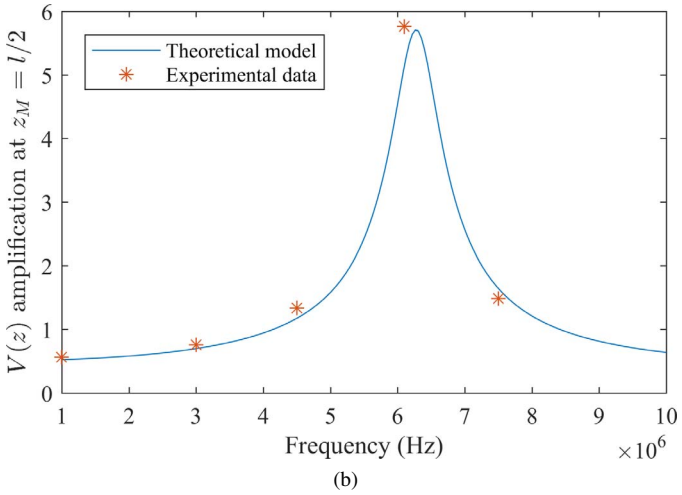

(b)

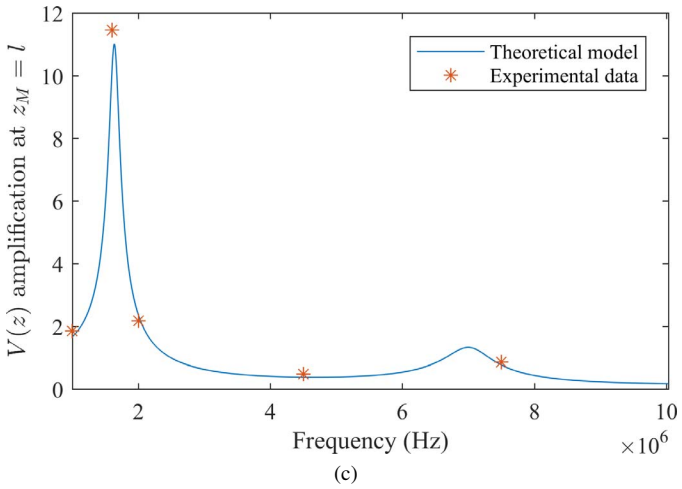

(c)

Fig. 4: Comparison of frequency-model results and experimental data for a two-conductor line ended with an (a) open circuit, (b) short-circuit and (c) parallel LC load

Source: http://www.caledonian-cables.co.uk

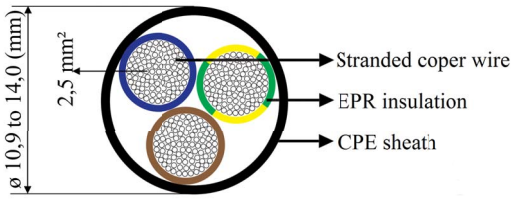

Fig. 5: Cross-section of the three-conductor cable used in the resonance experiment

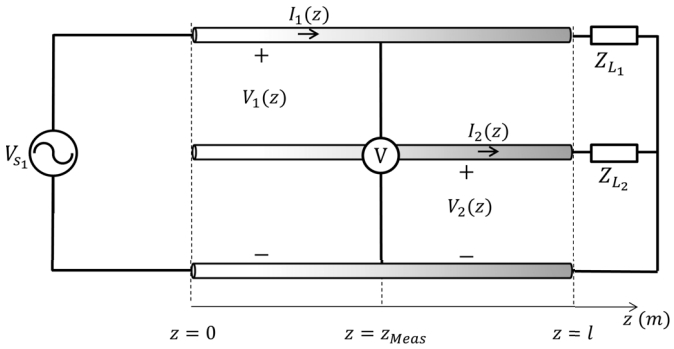

Fig. 6: Schematics of the connections made for three-conductor line resonance experiment

4c shows an equally high amplification in a line connected to a reactive load that may actually represent a passive device. This amplification takes place at line's endpoint for the chosen load. As an example, consider the case where the source emulates a polluting device, such as a power converter. The high frequency parasites on the load terminals may be up to 11 times higher than the injected harmonics, which in the worst case means they might be 11 times higher than the CISPR/IEC/ISO standards-established limits for the frequency bands around the resonance frequencies.

For the short-circuited line the voltage is minimal at the line's extremity, a configuration that is kept for resistive loads lower than $|Z_c|$. However, this configuration is not less dangerous because the load may still be affected by high frequency parasitic currents, considering that when a voltage minimum occurs at line extremities a current maximum arises at the same point [13].

B. Losses impact on resonance

As for any physical system that may be excited on its natural frequencies, the losses are the only factor restricting the resonant vibrations amplitudes. In the present case the losses are linked to the line per-unit-length series resistance R and parallel conductance G. Fig. 8 shows the maximal voltage amplification along the line for different values of R and G, illustrating the reduction of resonance amplitude as losses increase.

Naturally, if a resistive load is connected to the line's extremity it also interferes on the resonant voltage amplitude, but not only because the increase of system losses. Remind that when $Z_L = Z_c$ the line is adapted and resonance does

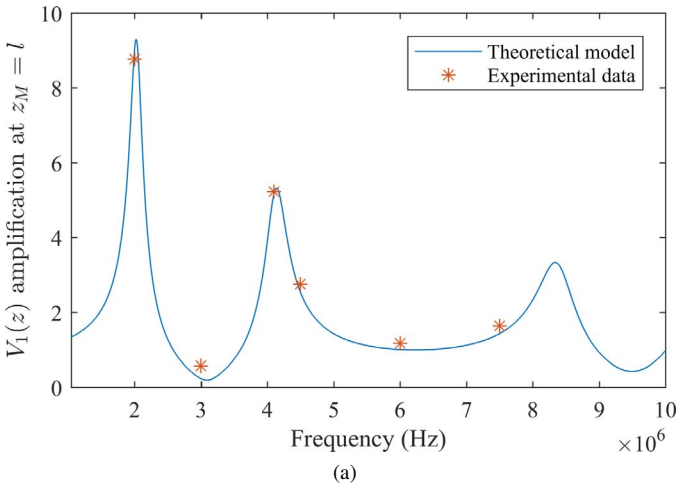

(a)

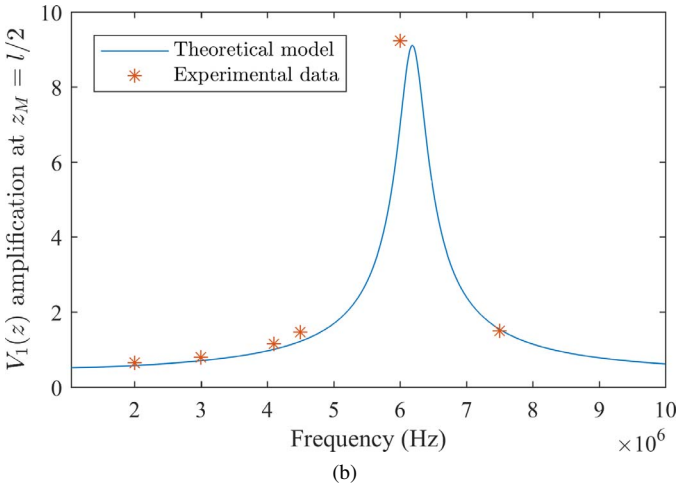

(b)

Fig. 7: Comparison between frequency-model results and experimental data for (a) two extremities short-circuited, third on air and (b) completely short-circuited three-conductor line

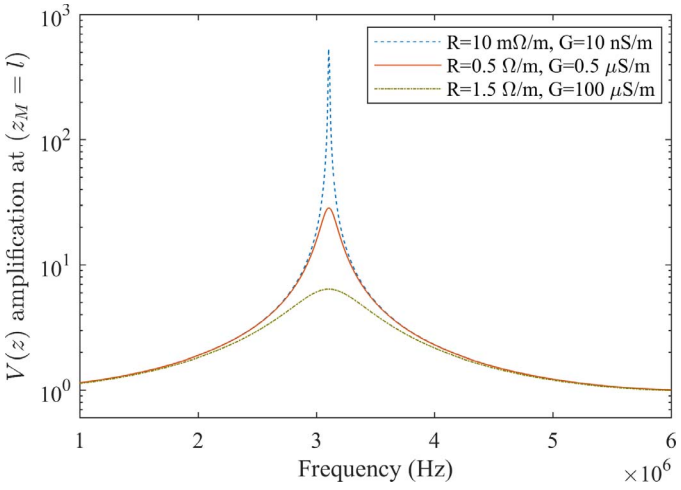

Fig. 8: Resonance-due voltage amplification for different loss-related parameters

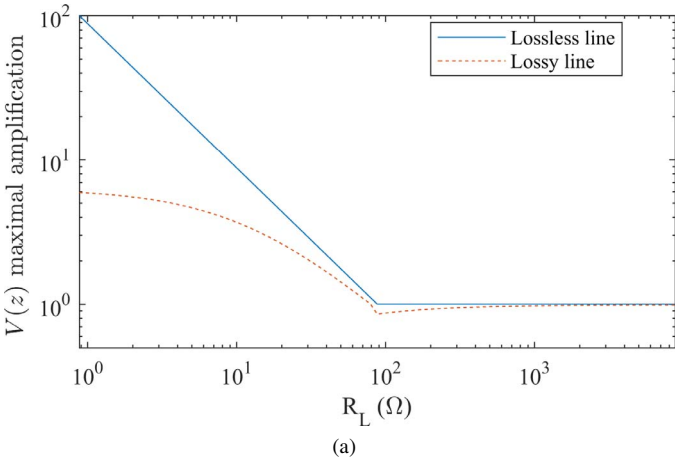

(a)

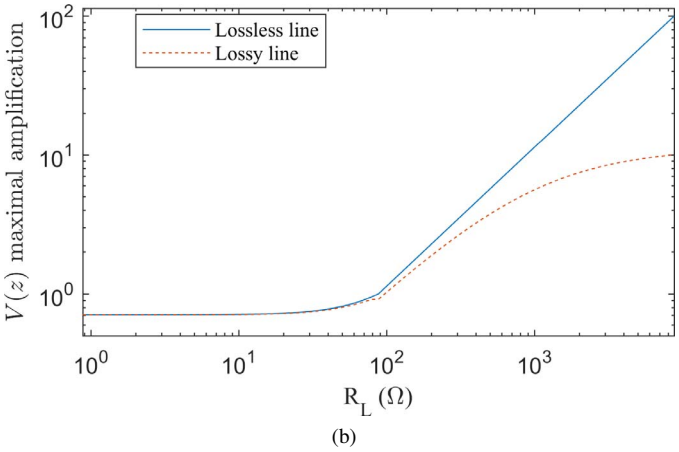

(b)

Fig. 9: Maximal voltage amplification along the two-conductors line at (a) $f = 6.333MHz$ and (b) $f = 3.167MHz$

not occur. Moreover, when Z_L is close to Z_c the voltage amplification due to resonance drops considerably. Therefore, the line losses impact on the resonance will be less evident the closer the load gets to the absolute value of the line's characteristic impedance Z_c. This behavior is illustrated on Fig. 9, where the maximal voltage amplification along the two-conductor cable is represented for different values of $Z_L = R_L$, at the fixed frequencies $f = 3,167MHz$ (open-circuit resonance frequency) and $f = 6,333MHz$ (short-circuit resonance frequency).

C. Amplification bandwidth

This section considers the probability of a power converter switching harmonic to excite the line at frequencies that will be dangerously amplified by the resonance phenomena.

On industrial applications, the maximal harmonic amplification supported by the load will depend only on the device's sensitivity. But, for a generic analysis, the classical definition of the half-power bandwidth is considered [13] and consists, in short, on the frequency band in which the line input power is superior than half of the maximum power demanded by the line (on resonance). The half-power bandwidth is drawn for the two-conductor line with parallel LC load in Fig. 10.

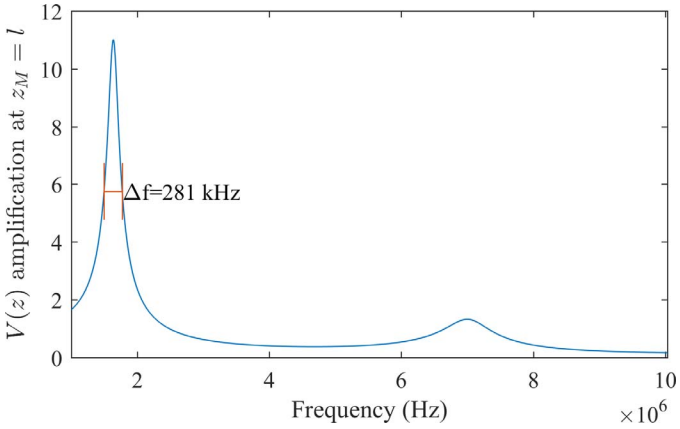

Fig. 10: Half-power amplification bandwidth,for the two-conductor line with parallel LC load.

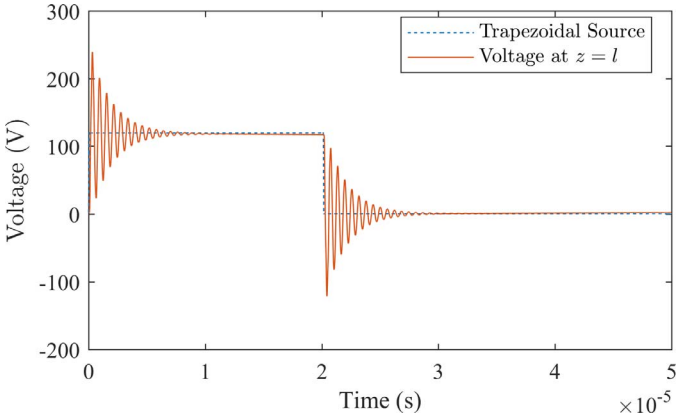

Fig. 11: Input trapezoidal source and correspondent voltage waveform at line's endpoint for two-conductor line with parallel LC load.

A bandwidth of $281kHz$ was obtained. Generally, the switching frequency of the power converters available goes up to $100kHz$, which means that switching harmonics will surely excite the line inside its amplification bandwidth.

The problems these harmonics can raise are discussed with the time-domain application in the next section

IV. Time-domain Application

The work presented in [9], [10] allows a representation of the switching cell output voltage by periodical trapezoidal ideal sources. We considered the simple case of a two-conductor line, the same used in our experiments, feed by a switching cell that may represent a voltage source inverter for example, having the parallel LC load described earlier in this paper as its load. The voltage on the switching cell output can be easily approximated by a trapezoidal source, its temporal form represented in dashed line in Fig. 11. The solid line in the same figure corresponds to the time-domain voltage at $z = l$, i.e. the load terminals, obtained from the conversion to time-domain of our frequency-domain solution.

These results agree with the work presented in [1], which shows that the over-voltages in the terminals of an electrical motor feed by a long cable directly connected to a voltage source inverter oscillates on the cable's natural frequency.

It is interesting to note that these harmonics present a problem only if they cannot be neglected at the first line resonance frequency. Considering that the Fourier series components of a trapezoidal signal can be neglected for frequencies higher than $1/t_r$, where t_r is the trapeze rise time, it can be established that dangerous resonance-due over-voltages will not occur if $t_r >> 1/f_n$.

V. Conclusion

In this paper a frequency-domain cable modeling capable to predict accurately the resonance frequency and voltage amplification was presented, as well as its time-domain transformed results. This tool can be used to predict potentially dangerous over-voltages on systems containing power-converters connected to electrically long cables, and therefore can be used to conceive more efficient protection techniques.

References

[1] H. Akagi and I. Matsumura, "Overvoltage mitigation of inverter-driven motors with long cables of different lengths," *IEEE Trans. Ind. Appl.*, vol. 47, jul/aug 2011.

[2] A. F. Moreira and T. H. Lipo, "High-frequency modeling for cable and induction motor overvoltage studies in long cable drivers," *IEEE Trans. Power Electron.*, vol. 25, oct 2002.

[3] H. D. Paula, D. A. de Andrade, M. L. R. Chaves, J. L. Domingos, and M. A. A. de Freitas, "Methodology for cable modeling and simulation for high-frequency phenomena studies in pwm motor drives," *IEEE Trans. Power Electron.*, vol. 23, mar 2008.

[4] L. Wang, C. N.-M. Hon, F. Canales, and J. Jatskevich, "High-frequency modeling of the long-cable-fed induction motor drive system using tlm approach for predicting overvoltage transients," *IEEE Trans. Power Electron.*, vol. 25, oct 2010.

[5] X. Chu, F. Lin, and Z. Yang, "The analysis of time-varying resonances in the power supply line of high speed trains," in *International Power Electronics Conference*, 2014.

[6] S. Zhang, S. Jiang, X. Lu, B. Ge, and F. Z. Peng, "Resonance issues and damping techniques for grid-connected inverters with long transmission cable," *IEEE Trans. Power Electron.*, vol. 29, jan 2014.

[7] M. C. Sousounis, J. K. H. Shek, and M. A. Mueller, "Filter design for cable overvoltage and power loss minimization in a tidal energy system with onshore converters," *IEEE Trans. Sustain. Energy*, vol. 7, jan 2016.

[8] M. Kuschke and K. Strunz, "Transient cable overvoltage calculation and filter design: application to onshore converter station for hydrokinetic energy harvesting," *IEEE Trans. Power Del.*, vol. 28, jul 2013.

[9] B. Revol, J. Roudet, J.-L. Schanen, and P. Loizelet, "Emi study of three-phase inverter-fed motor drives," *IEEE Trans. Ind. Appl.*, jan/feb 2011.

[10] R. Scheich, J. Roudet, S. B. t, and J. P. Ferrieux, "Common mode rfi of a hf power converter : Phenomena,its modelling and its measurement," in *EPE'93*, 1993.

[11] C. Paul, *Analysis of multiconductor transmission lines*. IEEE Press, 2008.

[12] J. Knockaert, J. Peuteman, J. Catrysse, and R. Belmans, "A vector impedance meter method to characterize multiconductor transmission-line parameters," *IEEE Trans. Electromagn. Compat.*, vol. 52, nov 2010.

[13] W. C. Johnson, *Transmission lines and networks*, first edition ed. McGRAW book company, 1950.